System Identification: An experimental verification

by R. D. Ciskowski

C. H. Liu

H. H. Ottesen

S. U. Rahman

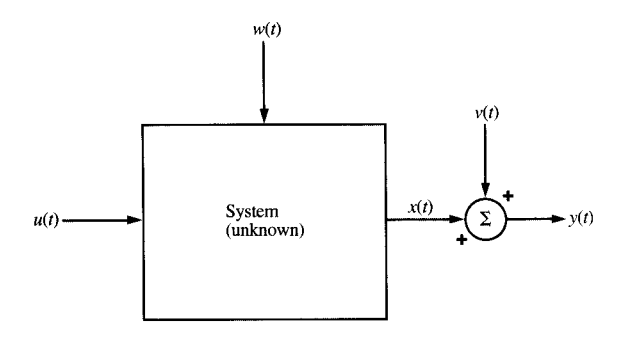
System Identification may be defined as the process of determining a model of a dynamic system using observed system input-output data. The identification of dynamic systems through the use of experimental data is of considerable importance in engineering since it provides information about system parameters which is useful in predicting behavior and evaluating performance. Traditional methods of System Identification are usually timeconsuming, costly, and difficult to use in other than a product development environment. Within the last decade, more sophisticated techniques for System Identification have been developed that can simultaneously estimate many parameters accurately and repeatedly. These modern techniques are, in addition, efficient, easy to use, inexpensive, and readily adaptable to manufacturing and in-the-field environments where they can be used to evaluate product quality and performance. This paper describes the use of one such System Identification algorithm to estimate several mechanical parameters of 8-inch hard-disk drive spindles in a manufacturing-like setting. The results obtained are in excellent agreement with results acquired by more conventional methods, and demonstrate the potential benefits of System Identification techniques in evaluating product quality and performance.

[®]Copyright 1987 by International Business Machines Corporation. Copying in printed form for private use is permitted without payment of royalty provided that (1) each reproduction is done without alteration and (2) the *Journal* reference and IBM copyright notice are included on the first page. The title and abstract, but no other portions, of this paper may be copied or distributed royalty free without further permission by computer-based and other information-service systems. Permission to *republish* any other portion of this paper must be obtained from the Editor.

Introduction

System Identification is a method of estimating the polynomial coefficients in the transfer function G(z) of an unknown system. The coefficient estimates are obtained by algebraically manipulating input $\{u(k)\}\$ and corresponding output response $\{y(k)\}\$ data sequences of that system. The unknown physical parameters (e.g., an electromechanical system would have force constant, friction, time constant, etc.) can then be found since they are functions of the estimated polynomial coefficients. System Identification methodology is finding applications in many fields of endeavor such as engineering, physical and life sciences, and economics. There are many advantages to using System Identification techniques. Unlike conventional methods for determining system parameters, which often require a series of different measurement settings, System Identification methods can determine all the parameters from a single measurement setting. This implies that all the estimated parameters are obtained under the same experimental conditions. As another advantage, conventional methods are often difficult, time-consuming, and costly, whereas System Identification can be performed quickly, easily, and inexpensively.

With this strong motivation, an experimental verification of System Identification was done on the motor-spindle-disk rotational assembly of 8-inch Direct Access Storage Devices (DASD) or hard-disk files. This paper describes the modeling and experimentation aimed at using System Identification techniques to identify several significant mechanical parameters of numerous DASD spindle assemblies. The estimated parameters obtained from this new method were compared with those obtained by conventional parameter measurement methods, and the results show that they are in excellent agreement.



Fleure

System Identification model: u(t) = input signal, x(t) = output signal from unknown system, w(t) = disturbance noise (plant noise), v(t) = observation noise (measurement noise), and y(t) = measured output signal.

System Identification background

System Identification, in the classical sense, has been around for a long time. It is commonly used to obtain system models or measure system performance directly from system (plant) data. Some of these classical methods of System Identification are

- Frequency response method (Bode plots).
- Step response method.
- Impulse response method.

Each of these traditional methods is basically used to obtain the system performance and the transfer function G(s) [or G(z)] by exciting the system with a known input and observing the corresponding output response.

The modern methods of System Identification refer to the process of constructing models and estimating (identifying) the best values of unknown system parameters from experimental input/output data. In this paper, we refer to System Identification techniques of the modern kind. We also assume that the models will be valid for linear, time-invariant, single-input/single-output, and stationary systems.

A typical model for System Identification is shown in **Figure 1**. The model of the unknown system is determined from the stored records of the input, u(t), and the corresponding output response, y(t).

The significant problems that must be addressed in System Identification are the following:

• Determination of the *order* of the model. The model should not be too complex to be understood and, thereby, incapable of predicting the dynamic behavior of the

unknown system. At the same time, it must not be trivial to the extent that predictions of dynamic behavior of the system become grossly inaccurate.

- Selection of the input signal u(t) which will maximize the
 accuracy of estimated parameters of the model. It is
 important that u(t) be sufficiently rich in frequency
 content to excite all modes of the unknown system.
- Selection of the suitable criterion for determining the model accuracy.
- Selection of *sampling time T* for use in numerical computation.

In spite of the fact that a great deal of work has been done in System Identification, we have at present no general answers to these questions.

Identification schemes that are available can be classified according to the manner in which they address some of the questions mentioned above, that is, the order of the model, input signal, and criterion used. In addition, it might also be of interest to classify them with respect to their implementation from a data processing standpoint. It might be sufficient to do all computations off-line (batch processing) after completion of measurements, or on-line computation might be required at the same time measurements are made.

The discrete-time transfer function G(z) of a linear system with samplers and zero-order-hold (ZOH) shown in **Figure 2** can be expressed as

$$G(z) = \frac{Y(z)}{U(z)} = (1 - z^{-1})Z \left[\frac{G(s)}{s} \right]$$

$$= \frac{b_1 z^{-1} + b_2 z^{-2} + \dots + b_n z^{-n}}{1 + a_1 z^{-1} + a_2 z^{-2} + \dots + a_n z^{-n}},$$
(1)

where the a_i 's and b_i 's ($i = 1, 2, \dots, \hat{n}$) are polynomial coefficients of the denominator and numerator, respectively, and $Z[\cdot]$ is the Z-transform operator; \hat{n} is the estimated order of the system.

The System Identification process is simply an algorithmic manipulation of the sampled input sequence $\{u(k)\}$ and its corresponding output response sequence $\{y(k)\}$. The results of this algorithmic procedure are the estimated values of the polynomial coefficients given in Equation (1). The process is conceptually shown in Figure 2.

We do not go into detail on the theory of System Identification and the great variety of algorithms that are available. There are several excellent texts available on these subjects [1-3].

The Least Squares (LS) System Identification algorithm [1] was tried first on the spindle motor input/output sequences to obtain estimates. The LS estimates, however, did not converge well at all. We attributed this to correlated noise (pink noise) contamination in the output sequence, and non-white noise, which is the basis for the LS algorithm. It was, therefore, necessary to select another algorithm that

would pre-whiten the pink noise in order to obtain a better convergence in the estimates.

The algorithm used for the experimental verification of System Identification was the Recursive Prediction Error Method (RPEM), which is similar to the Maximum Likelihood Estimate Method. This algorithm uses an ARMAX (Auto-Regressive Moving Average with Exogenous Variables) model, and its parameter estimates are quite robust with respect to plant and measurement noise. The computations were done in an off-line mode. The RPEM is briefly covered later, but a detailed discussion can be found in [3]. The derivations and applications of RPEM algorithms for different state-space representations have been extensively covered in References [3–10]. It would be almost impossible to address all the applications in this paper.

The strength of RPEM parameter estimation schemes is that they in fact prewhiten the noise and are thus asymptotically efficient when convergent. More significant perhaps is the fact that they can exploit effectively *a priori* knowledge concerning the signal models, such as knowledge of signal limiting from the plant. Moreover, RPEM schemes use lower-order dimensional parameter space than other identification schemes (i.e., extended least squares), and through suitable parameterizations, one can expect that this will contribute to better convergence.

The recursive prediction error methods are computationally complex and may converge to a local minimum of the prediction error cost function which may not be the global minimum, or may diverge and cause closed-loop instability.

A summary of a modified RPEM algorithm (see Appendix A for symbols and notation, and Appendix B for the algorithm) checks the stability of the dynamic system and is capable of detecting the outliers. (Outliers are measurement values that deviate substantially from other values in the measurement sequence.)

The spindle model

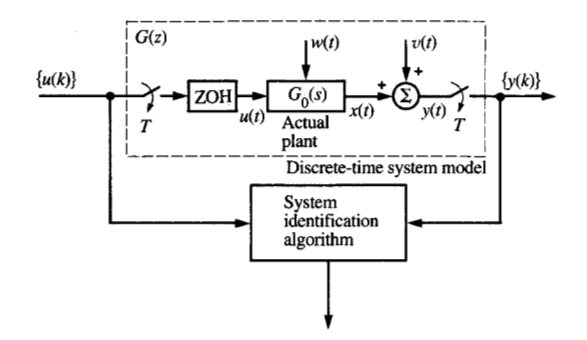
Before applying System Identification techniques on actual disk drives, we first experimented on a test-stand version of the spindle-motor-disk assembly as shown in **Figure 3**. On the basis of the dynamics of two rotational inertias J_1 and J_2 , we can develop differential equations governing the motion and arrive at a transfer function, $G_1(s) = \omega_2(s)/\tau(s)$, relating the output angular speed to the input torque in the s-domain. Here $\omega_2(s) = \dot{\theta}_2(s)$.

The two basic equations of spindle-motor-disk assembly in the time domain are

$$J_{1}\ddot{\theta}_{1}(t) + K[\theta_{1}(t) - \theta_{2}(t)] = \tau(t),$$

$$J_{2}\ddot{\theta}_{2}(t) + B\dot{\theta}_{2}(t) + K[\theta_{2}(t) - \theta_{1}(t)] = 0.$$
(2)

Using the state-variable representation, let us define the states $X_1(t)$ and $X_2(t)$ as follows: $X_1(t) = \theta_1(t)$, $X_3(t) = \theta_2(t)$,



Eleme /

The System Identification process: T = sampling period; ZOH = zero-order-hold; $(\hat{a}_1, \hat{a}_2, \dots, \hat{a}_n, \hat{b}_1, \hat{b}_2, \dots, \hat{b}_n \text{ estimated parameters.}$

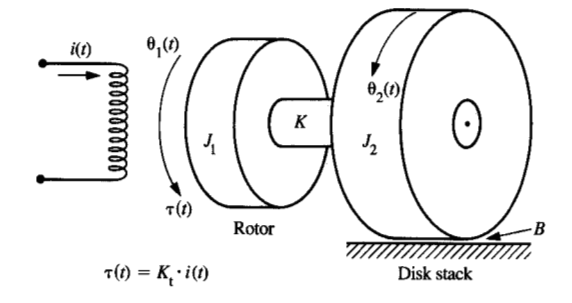


Figure (

Model of the test-stand assembly: $J_1 = \text{moment of inertia of the rotor}$, $J_2 = \text{moment of inertia of the disk stack}$, K = torsional stiffness coefficient, B = damping coefficient, $\tau(t) = \text{applied torque}$, $\theta_1(t) = \text{angular displacement of rotor}$, and $\theta_2(t) = \text{angular displacement of disk stack}$.

and the input torque as $U(t) = \tau(t)$. The angular velocity then becomes $\dot{X}_1(t) = \dot{\theta}_1(t) = X_2(t)$ and $\dot{X}_3(t) = \dot{\theta}_2(t) = X_4(t)$. Equations in (2) can also be written in matrix notation (indicated in boldface):

$$\dot{\mathbf{X}}(t) = \mathbf{F} \cdot \mathbf{X}(t) + \mathbf{G} \cdot U(t),$$

$$\mathbf{Y}(t) = \mathbf{H} \cdot \mathbf{X}(t),$$
(3)

573

where

$$\mathbf{F} = \begin{bmatrix} 0 & 1 & 0 & 0 \\ -K/J_1 & 0 & K/J_1 & 0 \\ 0 & 0 & 0 & 1 \\ K/J_2 & 0 & -K/J_2 & -B/J_2 \end{bmatrix} = \begin{bmatrix} 0 & 1 & 0 & 0 \\ -A_1 & 0 & A_1 & 0 \\ 0 & 0 & 0 & 1 \\ A_2 & 0 & -A_2 & -A_3 \end{bmatrix},$$

$$\mathbf{G} = \begin{bmatrix} 0 & 1/J_1 & 0 & 0 \end{bmatrix}^t = \begin{bmatrix} 0 & A_4 & 0 & 0 \end{bmatrix}^t,$$

$$\mathbf{X}(t) = \begin{bmatrix} X_1(t) & X_2(t) & X_3(t) & X_4(t) \end{bmatrix}^t,$$

where the superior t indicates the matrix transpose, and $A_1 = K/J_1$, $A_2 = K/J_2$, $A_3 = B/J_2$, and $A_4 = 1/J_1$. If we choose $\mathbf{H} = \begin{bmatrix} 0 & 0 & 1 & 0 \end{bmatrix}$, then the output becomes $y(t) = X_3(t)$, or the angular displacement of θ_2 . We have a so-called SISO (single-input/single-output) system. The open-loop transfer function is given by

$$G(s) = \frac{Y(s)}{U(s)} = \frac{\theta_2(s)}{\tau(s)} = \mathbf{H} [s\mathbf{I} - \mathbf{F}]^{-1}\mathbf{G}$$

$$= \frac{A_2 \cdot A_4}{s[s^3 + A_3 s^2 + (A_1 + A_2)s + A_1 \cdot A_3]},$$
(4)

where I is the identity matrix.

Since we are really measuring the disk-rotational (angular) velocity $\dot{\theta}_2(t) = \omega_2(\tau)$ as our output, both sides of Equation (4) are multiplied by s, yielding the third-order transfer function

$$G_{1}(s) = \frac{s\theta_{2}(s)}{\tau(s)} = \frac{\dot{\theta}_{2}(s)}{\tau(s)}$$

$$= \frac{A_{2} \cdot A_{4}}{s^{3} + A_{3}s^{2} + (A_{1} + A_{2})s + A_{1} \cdot A_{3}}.$$
 (5a)

The following estimated values of physical constants for the spindle test-stand are used:

$$J_1 = 2.23 \cdot 10^5 \text{ g-mm}^2,$$

 $J_2 = 4.26 \cdot 10^6 \text{ g-mm}^2,$
 $K = 1.34 \cdot 10^{12} \text{ g-mm}^2/\text{rad/s}^2,$
 $B = 10^5 \text{ g-mm}^2/\text{s}.$

Substituting these values into (5a), we have

$$G_{1}(s) = \frac{1.410}{s^{3} + 2.347 \cdot 10^{-2}s^{2} + 6.324 \cdot 10^{6}s + 1.141 \cdot 10^{5}}.$$
 (5b)

The three distinct roots of the denominator were determined, resulting in a real root, $a = -2.23 \cdot 10^{-2}$, and a pair of complex conjugate roots, $b \pm jc = -5.68 \cdot 10^{-4} \pm j2.51 \cdot 10^{3}$. Then the transfer function can be simplified to

$$G_1(s) = \frac{K_0}{(s+a)([s+b]^2 + c^2)},$$
(6)

where the numerator constant is $K_0 = 1.410$. The physical meanings of the coefficients can be interpreted as follows: $a \approx B/(J_2 + J_1) \approx B/J_2$ is the magnitude of the real dominant

mechanical pole, and $1/a \approx 44$ s is the mechanical time constant of the spindle-motor-disk assembly. The value c is the frequency of torsional resonance, which is in the neighborhood of 400 Hz for this test-stand system. And the magnitude of b determines the degree of damping of the resonance. The salient feature of this system is the large frequency separation between the torsional resonance poles at $-b \pm jc$ and the dominant motor pole at -a.

Preliminary spindle experiments

A series of preliminary System Identification experiments were performed on test-stand hardware closely resembling a hard-disk file stack and motor assembly. These experiments were used as a vehicle not only to test and debug hardware and software, but more importantly to determine the particular characteristics and peculiarities encountered when applying System Identification techniques to disk files.

The main components of the test apparatus consisted of the mechanical hardware needed to simulate a disk file, the necessary electrical controls, and an IBM PC for data acquisition.

To perform the System Identification experiments, the system dynamics would have to be excited in a frequency range affecting the parameters being identified, and both the input excitation and output response would have to be sampled to provide the time sequences used by the System Identification techniques. The excitation or input, u(k), to the system consisted of toggling the drive current to the motor between high and low values. The corresponding response output, y(k), was the average angular velocity per revolution of the rotor. This average velocity was determined using a digital counter, and a value was available for each revolution. The IBM PC acquired and stored the input and output time sequences. These were uploaded to a host VM system for further processing at the conclusion of an experiment.

The initial plan was to identify simultaneously the frequency of the mechanical torsional resonance, c, the amount of damping, B, and the torque constant, K_1 , of the motor; in other words, obtain all three values in a single identification process. However, some preliminary measurement and analysis had indicated that the torsional resonance of the mechanical system was around 560 Hz. The pattern of angular displacements (mode shape) between θ_1 and θ_2 at this resonance consisted of an out-of-phase rotation, and θ_1 on the motor side exhibited most of the angular motion due to the fact that $J_2 \gg J_1$. Therefore, at the operating rotational velocity (3100 rpm), it was extremely difficult to excite the torsional resonance so that it was measurable at the rotor (θ_2) or disk end.

On the other hand, in order to measure the damping coefficient and torque constant at operating rpm, the system would have to be excited in the frequency range of about 0.05 Hz, a four-order-of-magnitude difference with respect to

the 560-Hz torsional resonance. As a result, it would be impractical to provide the broadband excitation necessary to identify all three parameters simultaneously as originally intended

The results of these experiments indicated that two problem areas in the experimental procedure would need to be studied further and satisfactorily addressed before proceeding to additional experiments. The two problems were sampling delay and variable sampling rate.

The sampling delay problem occurred during the sampling of the angular velocity of the rotor. Because the sampled velocity was an average value, it was not the velocity occurring right at the time of the sample, but rather was delayed from that time by one-half the revolution time. Its effect on System Identification was shown to be insignificant. The variable sampling rate occurred because the spindle velocity was varied during the identification process. The length of the sampling period would, thus, vary with variation in the spindle velocity since the sampling was synchronized with a disk index marker. This problem, referred to as the nonsynchronous sampling problem, is discussed later.

Simplified model of the DASD dynamic spindle system

On the basis of the experimental knowledge gained from the test-stand system, we decided not to identify the higher-frequency mode due to torsional resonance, but to use the lower-frequency (0.05-Hz) excitation to identify the damping coefficient B and the motor torque constant K_1 . Thus, the overall system could be simplified to a first-order model by lumping J_1 and J_2 together and eliminating the torsional stiffness coefficient K. Again, we start with the differential equation

$$\tau(t) = K_{,i}i(t) = J\dot{\omega}(t) + B\omega(t), \tag{7}$$

where $\omega(t)$ is the rotational velocity of the spindle assembly and $J = J_1 + J_2$.

Rewrite (7) into the form $\dot{\omega}(t) = -(B/J)\omega(t) + (K_t/J)i(t)$. Let us define the state variable $X(t) = \omega(t)$, the input U(t) = i(t), and the output $Y(t) = \omega(t)$. Then we recognize this as a first-order system with the formula

$$\dot{X}(t) = -(B/J)X(t) + (K/J)U(t)$$

and the output equation

$$Y(t) = [1] \cdot X(t).$$

In the standard state-variable formulation, this is

$$\dot{\mathbf{X}}(t) = \mathbf{F}\mathbf{X}(t) + \mathbf{G}U(t),$$

$$\mathbf{Y}(t) = \mathbf{H}\mathbf{X}(t),\tag{8}$$

where we have $\mathbf{F} = [-B/J]$, $\mathbf{G} = [K_1/J]$, and $\mathbf{H} = [1]$.

The reduced-order open-loop transfer function $G_{\mathbb{R}}(s)$ of the simplified model is given by

$$G_{\mathbf{R}}(s) = \mathbf{H} \cdot [s\mathbf{I} - \mathbf{F}]^{-1} \cdot \mathbf{G}$$

$$= \frac{(K_{t}/J)}{(s + B/J)}.$$
(9)

Now, sampling the continuous-time transfer function $G_{\mathbb{R}}(s)$, using a zero-order-hold circuit, yields the discrete-time transfer function $G_{\mathbb{R}}(z)$. This is given by

$$G_{R}(z) = (1 - z^{-1})Z\left[\frac{G_{R}(s)}{s}\right]$$

$$= \frac{b_{1} \cdot z^{-1}}{1 + a_{1} \cdot z^{-1}},$$
(10a)

where

$$a_1 = -e^{-B \cdot T/J} \tag{10b}$$

and

$$b_1 = \frac{K_1 \cdot T}{R} (1 - e^{-B \cdot T/J}). \tag{10c}$$

Using the best-estimate values of a_1 and b_1 , the total spindle inertia J (which is assumed to be constant), and the sampling period T, we can easily determine the damping coefficient B and the torque constant K_1 of the spindle motor drive. Let us use \hat{a}_1 and \hat{b}_1 to denote the estimate results from the recursive identification scheme (RPEM). Thus, the estimate for the damping coefficient \hat{B} and the torque constant \hat{K}_1 can be found [Equations (10b) and (10c)] to be

$$\hat{B} = -\frac{J}{T} \cdot \ln\left(-\hat{a}_{1}\right) \tag{11}$$

and

$$\hat{K}_{t} = \frac{\hat{b}_{t} \cdot \hat{B}}{1 + \hat{a}}.\tag{12}$$

The nonsynchronous sampling problem

It has been mentioned that a problem of nonsynchronous or time-varying sampling periods was encountered in the test-stand experiments. This is a result of the method used to determine the file rotational velocity. The problem could have been eliminated by using expensive analog velocity transducers, but it was felt that there would be no comparable benefit to the parameter estimation accuracy of the System Identification for the increased expense. In the test-stand experiments, the effects of a variable sampling period were ignored. In order to obtain the accuracy required by System Identification in later experiments, the nonsynchronous sampling rate was accounted for, as is now described.

Figure 4 shows how the spindle velocity is measured. At the sensing of an index pulse, pulses from a constant-frequency oscillator are counted until the next index pulse occurs. Let N be the number of oscillator pulses counted between the file index pulses. The revolution time, then, is

575

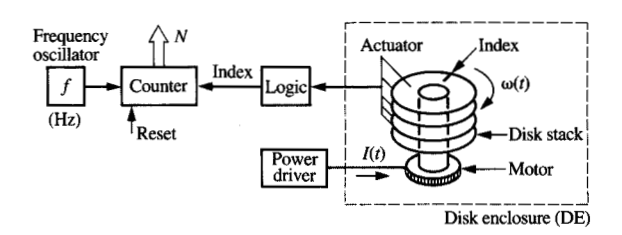
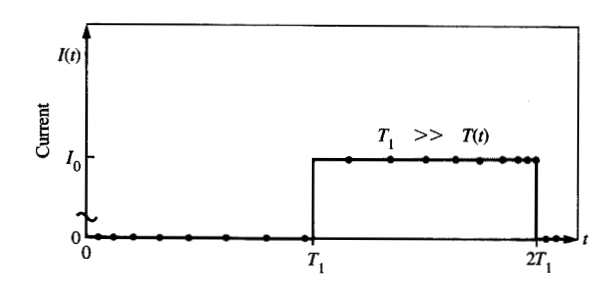


Figure 4

Typical method for obtaining spindle velocity measurements in hard-disk files.



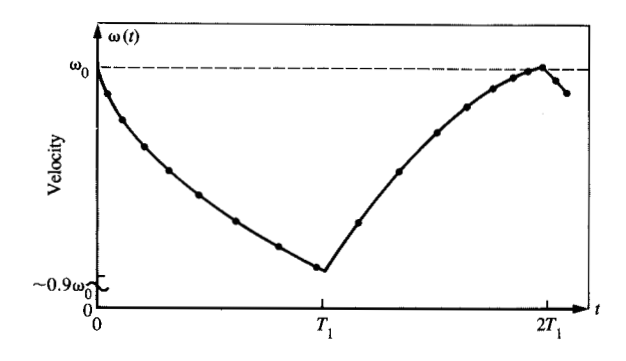


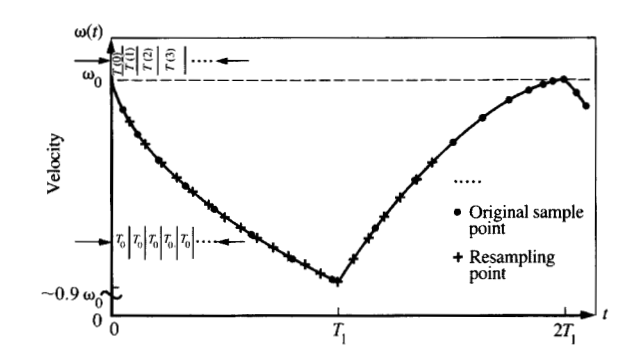
Figure 5

Nonsynchronous sampling of current and velocity

N/f, and the disk radian velocity is given by

$$\omega(t) = \frac{2\pi f}{N} [\text{rad/s}], \tag{13}$$

where f is the oscillator frequency.



Floure :

Graphical illustration of resampling process using the reconstructed velocity waveform.

The velocity in Equation (13) is the average angular velocity of the spindle in radians per second for that particular revolution. If the rotational velocity is *constant* and we repeat the process for each revolution, then the time between index pulses becomes a fixed sampling period T. However, if the velocity $\omega(t)$ changes, then the time between the index pulses also changes and we have a variable (nonsynchronous) sampling period T(t). The whole theory of System Identification is based upon a *constant* (fixed) sampling period T. Thus, for improved accuracy we adopted a "resampling" technique for the DASD spindle system identification.

In order for System Identification to be successful, the input u(t) must contain frequencies sufficient to excite the system dynamics. In the DASD spindle case, this was done open-loop by toggling the current as shown in **Figure 5**. The spindle rotational velocity would then increase and decrease. Correspondingly, the sampling periods would be timevarying. In Figure 5, it can be observed that the distance between sampling periods T(t) is variable. The toggling period T_1 is assumed to be much longer than the variable sampling period T(t).

The solution to this variable sampling period problem (see **Figure 6**) is to approximate the original velocity waveform in software by using a graphical interpolation between the nonsynchronous sampling points and then sample this new waveform at a constant sampling period. "Resampling method" is a good term to apply to this technique, since it is the second sampling process which occurs on the approximation of the velocity waveform. The resampling period T_0 is selected so that it is shorter than or equal to the minimum value of T(t).

The resampling method has successfully been tested on several DASD files with very good repeatability in estimating

values for the nonlinear drag coefficient B (around a steady-state velocity $\omega_0 \cong 2200$ rpm), and motor torque constant K_t . These values were obtained using the first-order system (n=1) with the discrete-time transfer function $G_R(z)$ expressed in Equation (10a).

The estimated values of a_1 and b_1 (i.e., \hat{a}_1 and \hat{b}_1) were obtained using the RPEM, with \hat{B} and \hat{K}_1 given by Equations (11) and (12), respectively. Note that B, the drag, is a nonlinear function of rotational velocity, so only small perturbations around ω_0 were permitted in order to be able to use a linear model as an approximation.

Experimental results using the RPEM

The System Identification experiments were performed on several 8-inch DASD files using the RPEM. The RPEM algorithm is quite robust against noise, as mentioned before, and has good parameter identification capabilities even in the presence of pink or filtered white noise. The convergence of the system parameters (a's, b's) depends upon selection of several key parameters (i.e., order of the system, order of the noise filter, and variable forgetting factors) for the RPEM.

The forgetting factor λ is a parameter which regulates how much the RPEM algorithm weights the past estimated parameter values Θ . λ can also be viewed as a time-varying data "smoother" where the length of the data to be smoothed increases exponentially with time. This time-varying weighting function depends upon the filter time constant α and initial and final values of the forgetting factor (i.e., λ_i and λ_∞ , respectively), and is given by the discrete equation

$$\lambda(k+1) = \alpha \cdot \lambda(k) + (1-\alpha)\lambda_{\infty},$$
with $\lambda(0) = \lambda_{i}$ and $\lambda(\infty) = \lambda_{\infty}.$

$$(14a)$$

Let the Z-transform of $\lambda(k)$ be $\Lambda(z)$; then Equation (14a) becomes

$$\Lambda(z) = \left(\frac{z}{z - \alpha}\right) \lambda(0) + \frac{(1 - \alpha) \lambda_{\infty}}{(z - \alpha) (1 - z^{-1})},\tag{14b}$$

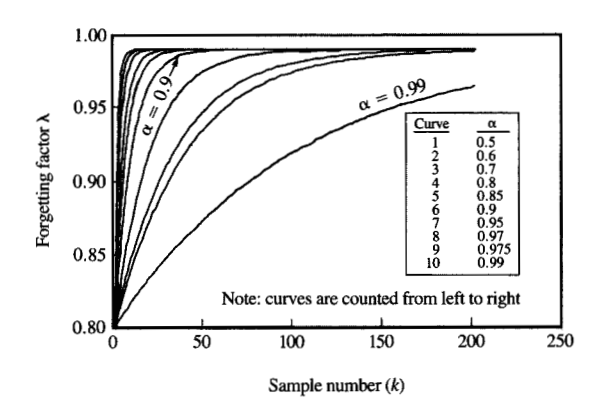
and the equation for the forgetting factor is

$$\lambda(k) = [\lambda(0) - \lambda(\infty)] \alpha^k + \lambda_{\infty}. \tag{14c}$$

The forgetting factor $\lambda(k)$ increases exponentially as time (or sample number k) elapses, and the rate of growth depends on the selection of time constant α . As shown in **Figure 7**, the initial value is set at $\lambda(0) = 0.8$, and the final value $\lambda(\infty) = 0.99$. When α is large (approaching unity), $\lambda(k)$ builds up slowly. However, when α is small (as $\alpha = 0.9$), $\lambda(k)$ grows much faster. It can be shown that the settling time is directly proportional to $-1/\log(\alpha)$.

The forgetting factor is also related to "memory size," given by

memory size
$$=\frac{1}{1-\lambda}$$
, (15)



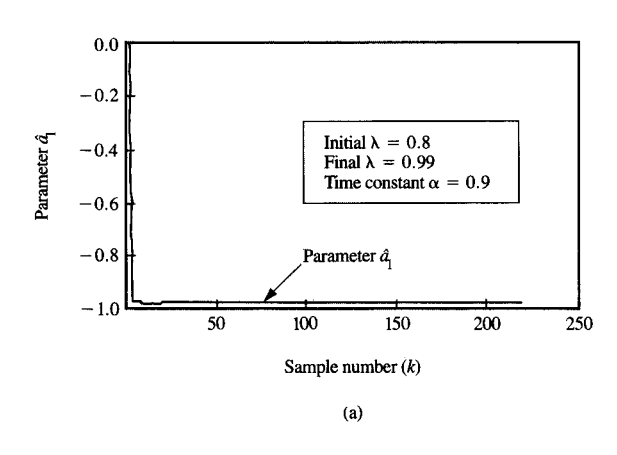
Floring

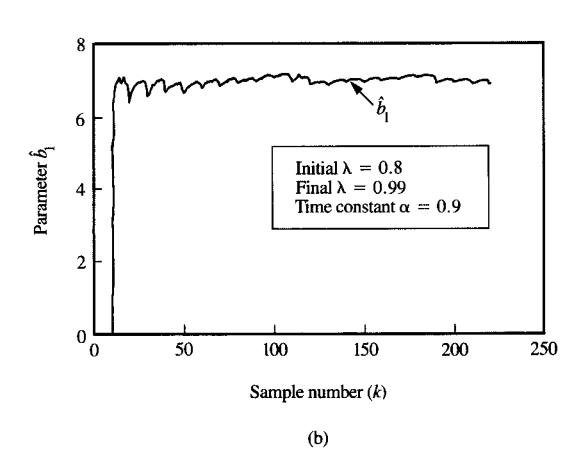
Forgetting factor (λ) versus number of samples (k) for different values of time constant (α) .

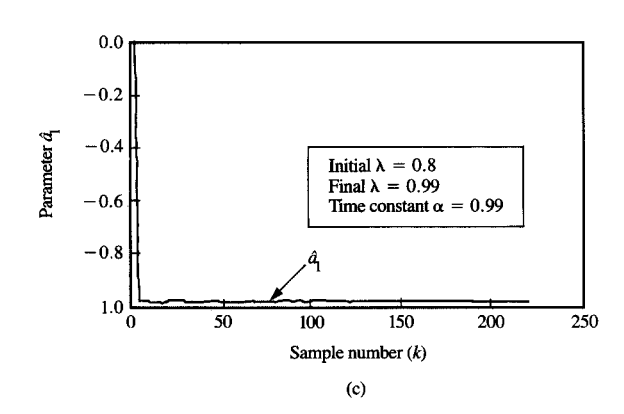
and corresponds to the number of past samples remembered; e.g., when $\lambda = 0.8$, the memory size = 5 samples, whereas when $\lambda = 0.9$, memory size increases to 10 samples to be processed. Therefore, the forgetting factor λ , with the time constant α , provides us with a useful tool for adjusting the sensitivity of the algorithm during the course of system identification.

The initial and final forgetting factors dictate the tracking of initial and final portions of the data sequence, respectively. The time constant α controls how fast $\lambda(k)$ builds up from the initial to the final values. Thus, at the start of a recursive process, we want a small value of $\lambda(k)$ which accounts for smaller numbers of samples to be remembered in order to compensate for the transience, or uncertainty, in the identification process. As time goes by, when the algorithm builds up confidence, we increase $\lambda(k)$ so as to include more samples to be calculated. In other words, small $\lambda(k)$ corresponds to "short-term" correction, and large $\lambda(k)$ is for "long-term" adjustment. Since there is no "cut-and-dried" method to determine how the forgetting factor filter should be designed, engineers need to experiment on their data with the algorithm to search for an optimal result.

The accuracy of the estimated parameters obtained using RPEM can be checked by observing the convergence of the parameters over time and comparing their values to those obtained by other measurement techniques. The selection of the order (m) of the pre-whitening noise filter was done by trial and error. The difference in parameter convergences between using a first-order and a second-order noise filter was very small. A first-order noise filter (m = 1) was, therefore, selected in the RPEM algorithm. Note that this







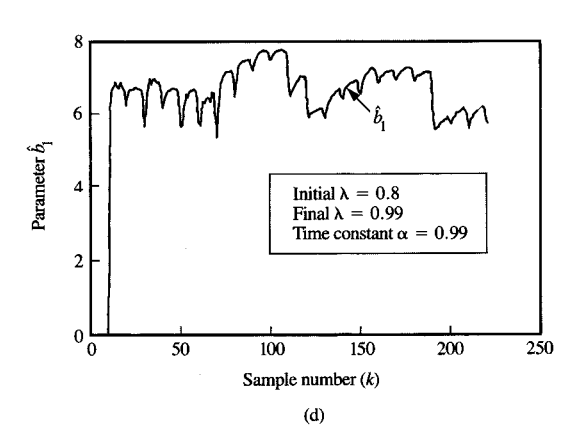


Figure 8

Convergence of \hat{a}_1 and \hat{b}_1 estimates versus number of samples (k) for time constant (a): (a) \hat{a}_1 for $\alpha = 0.9$; (b) \hat{b}_1 for $\alpha = 0.9$; (c) \hat{a}_1 for $\alpha = 0.99$; (d) \hat{b}_1 for $\alpha = 0.99$.

implies that c_1 in Equation (B3) of Appendix B is nonzero, and all other c's are equal to zero. The RPEM application program was designed in such a way that time-sequence records of the parameter estimates versus iteration number k were stored. This allowed sequential plotting of the parameter estimates shown in Figure 8.

The other key parameters $(\lambda_i, \lambda_\infty, \alpha)$ to be used in the RPEM should be selected so as to ensure adequate convergence. For the experimental data presented later, $\lambda_i = 0.8$, $\lambda_\infty = 0.99$, and $\alpha = 0.9$ were used as variable forgetting factor parameters. The convergence of the estimated parameters \hat{a}_1 and \hat{b}_1 is shown in Figures 8(a) and 8(b), which indicate that the \hat{a}_1 parameter converges much faster than the \hat{b}_1 parameter. The \hat{b}_1 parameter is related to the gains of the system and is more sensitive to changes in the input. The time constant α is also a critical parameter

which indirectly affects the convergence of the estimated parameters. The impact of changing α from 0.9 to 0.99 on convergence of the estimated parameters is shown in Figures 8(c) and 8(d). Inspection of these figures shows that the \hat{b}_1 parameter is still varying widely near the end of measurement. It also indicates the robustness of the \hat{a}_1 parameter even while the \hat{b}_1 parameter is not converging.

In Figure 8(b) [and to a large extent in Figure 8(d)] "blips" can be seen in the estimated b_1 sequence. These blips have a periodicity of ten samples (iterations), which corresponds to the periodicity of the on/off switching of the spindle motor current. These blips or disturbances in the b_1 estimate are probably due to nonlinear and/or higher-order effects in the actual spindle motor caused by "large" and fast motor current changes. The blips can be seen from the graphs to disturb the convergence. To minimize the blip effects, an

average over the last 20 b_1 -sequence points was taken to yield a final value for the b_1 estimate in Figure 8(b).

Summary of results

System Identification experiments were conducted using ten 8-inch hard-disk files. The file population consisted of both single and dual actuator units. A total of 78 individual measurements were made using these ten files. For each file, several distinct measurements were made during a one- to two-hour time frame, and this process was repeated several times over a four-month span. *Synchronous* sampling was used for all measurements.

Each System Identification measurement consisted of applying the System Identification algorithm to input and output data sequences from the file. This process yielded estimates of three specific file parameters, namely the estimated mechanical time constant $\hat{T}_{\rm m}$, the estimated damping coefficient \hat{B} , and the estimated dc gain constant \hat{G}_0 .

The time constant for the disk assembly of a hard file is a measure of the ability of the system to respond to dynamic input. The conventional method of determining the time constant is by measuring the rate of exponential decay of the angular velocity during spin-down from some initial value to 0.368 times this initial value. The mechanical time constant T_m is given by

$$T_{\rm m} = \frac{J}{B},\tag{16}$$

and the estimated mechanical time constant becomes

$$\hat{T}_{\mathsf{m}} = \frac{J}{\hat{B}}.\tag{17}$$

Note that the total inertia is treated as constant (a good assumption).

The estimated damping coefficient \hat{B} includes bearing drag, viscous drag on the disk surfaces, drag due to airflow pumping through the hub, and drag on the disks due to the presence of read/write heads. In the System Identification algorithm, the damping coefficient estimate is expressed by

$$\hat{B} = -\frac{J}{T_0} \cdot \ln\left(-\hat{a}_1\right). \tag{18}$$

The damping coefficient is usually not determined for a file by conventional methods. Instead, a related parameter, drag torque, is usually measured. The estimated drag torque $\hat{\tau}_d$ is derived using the estimated damping coefficient \hat{B} and the average angular spindle velocity ω_0 , i.e.,

$$\hat{\tau}_{d} = \hat{B} \cdot \omega_{0}. \tag{19}$$

The third parameter, dc gain, corresponds to the value of the Z-domain transfer function for the system evaluated at Z=1. In a more conventional setting, it can be determined analytically. The estimated dc gain \hat{G}_0 is given by

$$\hat{G}_0 = \frac{\hat{b}_1}{1 + \hat{a}_1}. (20)$$

These three parameters estimated by the System Identification algorithm were used along with the average angular velocity of the file during the measurement to derive estimates of two additional parameters, drag torque and torque constant. These two derived parameters, along with the time constant, give a direct measure of file performance having real physical significance for the engineer and are the three key results from the System Identification measurements. They are discussed here.

The estimated time constant was defined in (17). The drag torque $\tau_{\rm d}$ is the torque necessary to overcome all damping on the system. The torque constant is a measure of the ability of the file motor to provide torque to the system. The time constant, drag torque, and torque constant are important measures of file performance as well as of the quality of file components and the assembly process. System Identification provides all three parameters *simultaneously* without the need for special test fixtures.

The values of time constant, drag torque, and torque constant obtained from the System Identification measurements were found to be fairly *repeatable* from measurement to measurement for each particular file when operated under similar conditions. As an example, measurements on one particular single actuator file were repeated four times over a three-month time span. For these four groups of measurements, the estimated values of the time constant just after file start-up were 28.8, 31.0, 28.5, and 29.2 s.

Uniformity of the measurements from file to file was also evident from the data. The values obtained for each mechanical parameter were grouped within a fairly narrow range. For example, the time constant values for all *dual* actuator files were between 32 and 37 s.

Sensitivity of the measured parameters to changes occurring within a single file could be seen when the values of drag torque were examined over a group of file measurements made within a span of several hours. File warm-up occurs with each successive measurement, and this should reduce the amount of drag on the disk assembly because of decreased drag due to the bearings. This reduction can be seen in drag torque values as a reduction over time (see Figure 9). The parameters obtained from System Identification techniques, therefore, can successfully be used to flag changes occurring in the file over time.

The parameters can also be used as pass/fail criteria for the files. The torque-constant values were all grouped rather tightly around 0.035 N-m/A, except for one file which had a very low value. The low torque constant for this file indicated an inadequate drive motor. Closer examination revealed that this motor had difficulty starting the file. This critical difference was easily and quickly highlighted by the System Identification parameters. Therefore, specifications

0.04

Figure 9 Variation of drag torque over time for five files.

Table 1 Typical comparison of time-constant values obtained from System Identification and several conventional methods.

Estimates from System Identification	Estimates from conventional methods (s)		
	File coast-down	During System Identification	Analysis
30.2	30.0	30.8	33.1

Table 2 Typical comparison of drag torque values obtained from System Identification and analysis for three similar files.

Drag torque e. (N-m)	
System Identification	Analysis
0.0371	0.039
0.0364	0.034
0.0394	0.037

could be established for these parameters and used as pass/fail criteria for the files.

Closure

The verification of System Identification results on several hard files was done indirectly by comparing the estimates of the three parameters, time constant, drag torque, and torque constant, from System Identification measurements with values for these same parameters determined analytically and by independent experiments.

The estimated time constant obtained from System Identification was verified by comparing it with the values obtained by three other more conventional methods. The first method was a file coast-down experiment that consisted of measuring the time required for the file to slow from some initial rotational velocity to 0.368 times that value. The second method was similar to the first, but used data distinct from but available during a System Identification measurement to compute an estimate of the time constant. The third method was to obtain an analytical prediction of the value of the time constant. This was accomplished by estimating the rotational energy present in the file at operating rpm, determining the primary damping factors acting on the file, and then estimating the drag torque effects of these damping factors. An estimate of the time constant of the file could then be obtained by using the initial rotational energy and computing its decrease over time because of the presence of drag torque due to the damping factors. The comparison of the System Identification value with those obtained by the other three methods is summarized in Table 1. The comparison of values obtained from the experimentally based methods was very good. The analytically determined value was slightly higher. It must be stated that the three methods of estimating the time constant used here are the more conventional means of obtaining an estimate of this important parameter. They are timeconsuming and require a substantial amount of effort to conduct. The benefit of System Identification experiments is highlighted because of the ease with which the time-constant value can be determined for each file.

For drag torque verification, the values obtained from System Identification measurements were checked against analytically determined values based upon estimates of the drag torque due to the primary factors affecting file damping. **Table 2** presents several comparisons showing good agreement between the System Identification and the analytically computed values.

Excellent closure was also obtained for the torque-constant values determined by System Identification. Values obtained for specific files were compared with values of the motor torque measured experimentally on a test stand designed for this purpose. These test-stand measurements were made *before* the motors were installed in the files. The values are compared in **Table 3**, again showing excellent agreement. All the torque-constant values obtained from System Identification measurements except two were found to be within the specifications set for the file. One, already mentioned, had a very low value, while another had a slightly higher value than the specified range.

It is quite evident that the time-constant, drag torque, and torque-constant values estimated by System Identification

measurements exhibit excellent agreement with values obtained by more conventional methods. System Identification measurements provided *all three* values simultaneously, quickly, and easily, whereas the more conventional methods of estimating these parameters required three distinct, time-consuming efforts.

Conclusions

The main objective of the research described in the body of the paper was to gain experimental knowledge about identification of electromechanical system parameters and to compare the results with those of conventional methods for parameter estimation. The RPEM algorithm was chosen because of its robustness in the presence of non-white noise.

The closure between results obtained from the RPEM and the conventional estimation methods has been excellent. The sensitivity and repeatability of these RPEM parameter estimations were much better than those obtained from conventional methods. For the DASD spindle experiment, the nonsynchronous sampling problem was encountered and resolved with a novel solution, i.e., the resampling technique.

The results of these experiments show that System Identification is a viable tool for parameter estimation and may replace many time-consuming conventional methods for DASD spindles in the near future.

Although the experimental parameter identification was only applied to DASD spindles, it can easily be extended to linear and rotary DASD actuators as well as other electromechanical systems. While the described RPEM algorithm was run off-line, there are on-line parameter estimation methods that can be used in connection with adaptive control of electromechanical structures.

As the title of this paper indicates, this has been an experimental verification of the System Identification RPEM algorithm. The reader who is interested in the mathematical derivation of this algorithm can consult Appendix B or some of the listed references.

Acknowledgments

The authors would like to thank Dr. G. F. Franklin, Stanford University professor and consultant at IBM, Rochester, Minnesota, for bringing System Identification to life and outlining the RPEM algorithm.

Appendix A: Symbols, abbreviations, and notational conventions

A	Boldface capital letters indicate matrices		
\mathbf{A}^{t}	Transpose of matrix A		
\mathbf{A}^{-1}	Inverse of matrix A		
ARMAX	Auto-Regressive Moving Average with		
	Exogeneous Variables		
В	Damping coefficient		
DASD	Direct Access Storage Devices		

Table 3 Typical comparison of torque constant values from System Identification and test-stand measurements for four similar files

Motor torque constant range

System Identification		Test stand	
Minimum	Maximum	Minimum	Maximum
0.0340	0.0368	0.0363	0.0395
0.0339	0.0414	0.0360	0.0410
0.0347	0.0391	0.0362	0.0416
0.0333	0.0376	0.0359	0.0396

G(s)	Open loop transfer function in s-domain
G(z)	Discrete time transfer function (z-domain)
\hat{G}_{0}	Estimated dc gain of spindle motor
$G_{\mathbf{R}}(z)$	Reduced order discrete transfer function
I	Identity matrix
i(t)	Current
J	Total moment of inertia $J = J_1 + J_2$
$J_{_1}$	Moment of inertia of rotor
J_2	Moment of inertia of disk stack
K	Torsional stiffness coefficient
$K_{\rm t}$	Motor torque constant
$\mathbf{L}(k)$	Adaptation gain matrix
ln	Natural logarithm
ĥ	Estimated order of the system
$\mathbf{P}(k)$	Covariance matrix
RPEM	Recursive Prediction Error Method
SISO	Single-input/single-output
T	Sampling period
T_{0}	Resampling time period
\hat{T}_{m}	Estimated mechanical time constant
$\{u(k)\}$	Input sequence
V(t)	Measurement noise = $e(k) + \hat{c}_1 \cdot e(k-1)$
	$+\cdots \hat{c}_n e(k-n)$
$V_{\mathbf{n}}(\mathbf{\Theta})$	Loss function
$V_{n}(\mathbf{\Theta})$	First derivative of cost function with respect to Θ
$\ddot{V}_{\rm n}(\mathbf{\Theta})$	Second derivative of cost function with respect
	to Θ
W(t)	Process noise
$\{y(k)\}$	Output sequence
Z	Z-transform operator
ZOH	Zero-order-hold
α	Time constant for RPEM algorithm
$\alpha(k-1)$	
$\epsilon_{p}(k)$	Prediction error
$\bar{\epsilon}_{\rm p}(k)$	Residual prediction error
θ	Parameter matrix (vector)
ê	Estimated parameter matrix (vector)
$\theta_1(t)$	Angular position of rotor
$\theta_2(t)$	Angular position of disk stack

 $\lambda(k)$ Variable forgetting factor (lambda) λ_i Initial value of forgetting factor

 λ_{m} Final value of forgetting factor

 $\tau(t)$ Applied torque

 $\hat{\tau}_{d}$ Estimated drag torque

 $\phi'(k-1)$ Observed data matrix (vector) from past measurement

 $\overline{\phi}'(k-1)$ Sensitivity matrix (vector) using residual error

 $\psi(k-1)$ Sensitivity matrix (vector)

 $\overline{\psi}'(k-1)$ Observed data matrix (vector) using residual error

 $\omega(t)$ Angular velocity

 ω_0 Average angular spindle velocity

Appendix B: Parameter estimation with the RPEM algorithm (using residual error)

The intent of this appendix is to summarize the RPEM algorithm used for recursive identification of the simplified dynamic model. This improved algorithm has better convergence properties even for time-varying parameters in the presence of colored/pink noise. The "variable forgetting factor" given by the first-order difference equation

$$\lambda(k+1) = \alpha\lambda(k) + (1-\alpha)\lambda_{\infty}$$

was introduced to eliminate the influence of the old data and make the estimates insensitive to large measurement errors (outliers).

Consider a SISO system represented by the ARMAX model

$$A(z^{-1}) \cdot v(k) = B(z^{-1}) \cdot u(k) + C(z^{-1}) \cdot e(k),$$
 (B1a)

where z^{-1} is a backward shift operator and the polynomials $A(z^{-1})$, $B(z^{-1})$ and $C(z^{-1})$ are given by

$$A(z^{-1}) = 1 + a_1 \cdot z^{-1} + a_2 \cdot z^{-2} + \dots + a_n \cdot z^{-n},$$
 (B1b)

$$B(z^{-1}) = b_1 \cdot z^{-1} + b_2 \cdot z^{-2} + \dots + b_n \cdot z^{-n},$$
 (B1c)

$$C(z^{-1}) = 1 + c_1 \cdot z^{-1} + c_2 \cdot z^{-2} + \dots + c_m \cdot z^{-m},$$
 (B1d)

and e(k) is colored/pink noise. Assuming that the order (m) of the noise filter $\{C(z^{-1})\}$ and its estimated coefficient c's are known, the ARMAX model (B1a) can also be represented as

$$y(k) = \phi'(k-1)\Theta, \tag{B2}$$

where the parameter and observed data vectors are defined as

$$\Theta = [a_1 a_2 \cdots a_n, b_1 b_2 \cdots b_n, c_1 c_2 \cdots c_m]^t,$$
 (B3)

$$\phi'(k-1) = [-y(k-1) \cdots -y(k-n) \ u(k-1)$$

$$\cdots u(k-n)e(k) \cdots e(k-m)$$
]. (B4)

The objective is to come up with the best estimate of parameter vector denoted by $\hat{\Theta}(k)$,

$$\hat{\mathbf{\Theta}} = [\hat{a}_1 \hat{a}_2 \cdots \hat{a}_n, \hat{b}_1 \hat{b}_2 \cdots \hat{b}_n, \hat{c}_1 \hat{c}_2 \cdots \hat{c}_m]',$$

such that the weighted quadratic cost function in prediction error

$$V_n(\mathbf{\Theta}) = \sum_{k=1}^{N} \lambda^{N-k} \cdot [y(k) - \hat{y}(k)]^2$$
$$= \sum_{k=1}^{N} \lambda^{N-k} \cdot \epsilon_p^2(k), \tag{B5}$$

is minimized, using iterative numerical search procedures. *N* is the number of samples. A very common form of such a procedure (Gupta and Mehra) is

$$\hat{\mathbf{\Theta}}(k) = \hat{\mathbf{\Theta}}(k-1) - \alpha(k-1) + [\hat{\mathbf{V}}_{-} \{\hat{\mathbf{\Theta}}(k-1)\}]^{-1} \cdot \hat{\mathbf{V}}_{-} \{\hat{\mathbf{\Theta}}(k-1)\}, \quad (B6)$$

where sensitivity function \dot{V}_n is defined as a negative gradient of the prediction error and the Hessian matrix $\{P(k)\}$ is approximated as given:

$$\psi(k-1) = \dot{V}_{n} \{\Theta(k-1)\} = -\left[\frac{d\epsilon_{p}}{d\Theta}\right]^{r}$$

$$= \phi(k-1) - \{\hat{c}_{1}(k-1) \, \psi(k-2) + \cdots + \hat{c}_{m}(k-m) \, \psi(k-m+1)\}, \tag{B7}$$

$$\mathbf{P}(k)^{-1} = \ddot{V}_{n} \{ \mathbf{\Theta}(k-1) \}^{-1} \cong \sum_{n} \left[\frac{\partial \epsilon_{n}}{\partial \mathbf{\Theta}} \right]^{l} \left[\frac{\partial \epsilon_{n}}{\partial \mathbf{\Theta}} \right].$$
 (B8)

The prediction error is defined as

$$\epsilon_{\mathbf{n}}(k) = y(k) - \phi'(k-1)\hat{\mathbf{\Theta}}(k-1). \tag{B9}$$

The adaptation gain matrix is computed as

$$\mathbf{L}(k) = \frac{\mathbf{P}(k-1) \, \psi(k-1)}{\lambda \mathbf{I} + \psi'(k-1) \, \mathbf{P}(k-1) \, \psi(k-1)}.$$
 (B10)

The covariance matrix is updated as

$$\mathbf{P}(k) = \frac{1}{\lambda} \cdot [\mathbf{I} - \mathbf{L}(k)\psi'(k-1)] \cdot \mathbf{P}(k-1). \tag{B11}$$

The parameter vector is updated by the recursive relation

$$\hat{\mathbf{\Theta}}(k) = \hat{\mathbf{\Theta}}(k-1) + \mathbf{L}(k)\epsilon_{\mathbf{p}}(k). \tag{B12}$$

The stability test was also incorporated in the RPEM algorithm, which ensures that the polynomial $C(z^{-1})$ is stable and is capable of detecting outliers. The RPEM algorithm can be significantly improved by computing the "residual error," defined as

$$\bar{\epsilon}_{\rm p}(k) = y(k) - \phi'(k-1) \,\hat{\Theta}(k),$$

and substituting for prediction error to calculate observed and data vector and sensitivity vector given as

$$\overline{\phi}'(k-1) = [-y(k-1) \cdots -y(k-n) \ u(k-1) \cdots$$

$$u(k-n) \ \tilde{\epsilon}_n(k) \ \tilde{\epsilon}_n(k-1) \cdots \ \tilde{\epsilon}_n(k-m)], \qquad (B13)$$

$$\overline{\psi}(k-1) = \overline{\phi}(k-1) - \{\hat{c}_1(k-1) \cdot \psi(k-2) + \cdots \hat{c}_k(k-m) \cdot \psi(k-m+1)\}.$$
(B14)

A summary of the improved RPEM algorithm using residual error is given here to make the paper self-contained:

1. Select the initial values for RPEM algorithm parameters. Select also the order of noise filter $C(z^{-1})$ and its estimated coefficients:

$$P_0 = 10^6 \mathbf{I}, \ \lambda_i = 0.8, \ \lambda_{\infty} = 0.995, \ \alpha = 0.95,$$

 $\overline{\phi}(0), \ \overline{\psi}(0), \ \hat{C}_c, \text{ order of } C(z^{-1})$

- 2. Select the length of measurements N.
- 3. Compute the prediction and residual errors:

$$\epsilon_{p}(k) = y(k) - \phi'(k-1) \hat{\Theta}(k-1),$$

 $\tilde{\epsilon}_{n}(k) = y(k) - \overline{\phi}'(k-1)\hat{\Theta}(k).$

 Form the observed data matrix (vector) based on residual error:

$$\overline{\phi}^{\prime}(k-1)$$
.

- 5. Form the sensitivity vector based on residual error: $\mathbf{V}(k-1)$.
- 6. Compute the adaptation gain L(k):

$$\mathbf{L}(k) = \frac{\mathbf{P}(k-1)\,\overline{\boldsymbol{\psi}}(k-1)}{\lambda\mathbf{I} + \overline{\boldsymbol{\psi}}'(k-1)\mathbf{P}(k-1)\overline{\boldsymbol{\psi}}(k-1)}.$$

7. Update the covariance matrix P(k)

$$\mathbf{P}(k) = \frac{1}{\lambda} \cdot \left[\mathbf{I} - \mathbf{L}(k) \, \overline{\psi}'(k-1) \right] \cdot \, \mathbf{P}(k-1).$$

8. Update the parameter vector

$$\hat{\mathbf{\Theta}}(k) = \hat{\mathbf{\Theta}}(k-1) + L(k)\epsilon_{\mathbf{p}}(k).$$

9. Compute the innovation error

$$\bar{\epsilon}_{-}(k) = y(k) - \bar{\phi}'(k-1)\hat{\Theta}(k).$$

10. Increment k and go to 3.

References

- G. F. Franklin and J. D. Powell, Digital Control of Dynamic Systems, Addison-Wesley Publishing Co., Reading, MA, 1980.
- N. K. Sinha and B. Kuszta, Modeling and System Identification of Dynamic Systems, Von Nostrand Reinhold Co. Ltd., New York, 1983.
- 3. L. Ljung and T. Soderstrom, *Theory and Practice of Recursive Identification*, MIT Press, Cambridge, MA, 1983.
- G. C. Goodwin and K. S. Sin, Adaptive Filtering, Prediction and Control, Prentice-Hall, Inc., Englewood Cliffs, NJ, 1984.
- J. B. Moore and H. Weiss, "Recursive Prediction Error Algorithm Without a Stability Test," *Automatica* 16, 683–687 (1980).
- J. B. Moore and R. K. Boel, "Asymptotically Optimum Recursive Prediction Error Method in Adaptive Estimation and Control," *Automatica* 20, No. 2, 237-240 (1986).
- N. K. Sinha and F. K. Omani, "Modified Approach to State-Space Self-Tuning Control with Pole Assignment," *Proc. IEEE* 132, Pt. D, No. 6, 257–262 (November 1985).

- 8. J. K. Tugnait, "Recursive Parameter Estimation for Noisy Autoregressive Signals," *IEEE Trans. Info. Theory* IT-32, No. 3, 426-430 (May 1986).
- J. B. Moore and H. Weiss, "Recursive Prediction Error Methods for Adaptive Estimation," *IEEE Trans. Syst. Man. Cyber.* SMC-9, No. 4, 237-240 (April 1979).
- K. J. Astrom and B. Wittenmark, Computer Controlled Systems, Theory and Design, Prentice-Hall, Inc., Englewood Cliffs, NJ, 1984

Received August 8, 1986; accepted for publication April 13, 1987

Robert D. Ciskowski IBM System Products Division, Rochester, Minnesota 55901. Mr. Ciskowski joined IBM in 1982 at Rochester, Minnesota. He received a B.S. in mathematics and computer science from the University of Illinois at Urbana in 1971, a B.S. in mechanical engineering from the University of Texas at Austin in 1976, and an M.S. in mechanical engineering from North Carolina State University in Raleigh in 1980. His experience prior to joining IBM includes computer programming and engineering positions in industry as well as a term as a mathematics teacher in the Peace Corps. Within IBM, he has been concerned primarily with the development and analysis of mechanical components for hard-disk files. He is currently completing his Ph.D. dissertation in mechanical engineering at North Carolina State University through the IBM Resident Study Program. His dissertation research involves the boundary element method of analysis applied to scalar and vector wave propagation. Mr. Ciskowski is a member of the Acoustical Society of America, the American Society of Mechanical Engineers, and the Association for Computing Machinery.

Charles H. Liu IBM System Products Division, Rochester, Minnesota 55901. Mr. Liu received his M.S. in electrical engineering from the Massachusetts Institute of Technology, Cambridge, in 1975. Upon graduation, he worked on the impact printer design for NCR in Ithaca, New York. In 1977, he joined IBM in Rochester, and has worked on the design and development of disk drive products in both data and control channels. Mr. Liu is currently studying control sciences at the University of Minnesota under the IBM Resident Study Program. His interests include robust feedback control designs, computer-aided-design algorithms, and system identification.

Hjalmar H. Ottesen IBM System Products Division, Rochester, Minnesota 55901. Dr. Ottesen received his B.S. and M.S. in electrical engineering from the University of Colorado, Boulder, in 1961 and 1962. He joined IBM in San Jose, California, in 1962, working on data acquisition and control systems. In 1965 he went on an educational leave of absence, obtaining in 1968 a Ph.D. in electrical engineering under a full university fellowship grant from the University of Colorado. Dr. Ottesen has held various technical positions in advanced development of magnetic recording channels and position control systems for tape, disk, and mass storage devices at several IBM laboratories. He is currently a senior engineer in prototyping and file technology at Rochester. His activities and current interests include advanced disk file development and

teaching of digital control, parameter estimation, and system identification of electromechanical systems. Dr. Ottesen has been awarded three IBM Invention Achievement Awards. He is a senior member of the Institute of Electrical and Electronics Engineers and a member of Eta Kappa Nu and Tau Beta Pi.

Shafiq-Ur-Rahman IBM Systems Technology Division, 11400 Burnet Road, Austin, Texas 78758. Mr. Rahman received a B.Sc. degree in electrical engineering (with specialization in electronics and communication engineering) from the West Pakistan University of Engineering and Technology, Lahore, in 1978. He joined IBM in Rochester, Minnesota, in 1980, having received an M.S. in electrical engineering from the University of Wyoming, Laramie, in 1980. Until 1984, he had worked in manufacturing engineering (System Products Division) on the design of highly sophisticated computercontrolled testers to detect surface defects in DASD products. In 1984, he transferred to the research and development laboratory in Rochester, where he was involved in the design, development, and track misregistration modeling for the overall performance evaluation of 8-inch DASD files. In 1985, he transferred to the research and development laboratory (Systems Technology Division) in Austin, where he is involved in electrical characterization and coupled noise (crosstalk) analysis in second-level packaging applications. His research interests are currently focused on adaptive control and its applications to communication engineering and expert systems. Mr. Rahman is pursuing his doctorate in electrical engineering at the University of Texas, Austin.